Research Article/Civil and Sanitary Engineering http://doi.org/10.15446/ing.investig.99526

A New Methodology Based on Artificial Intelligence for Estimating the Compressive Strength of Concrete from Surface Images

Una nueva metodología basada en inteligencia artificial para estimar la resistencia a la compresión del hormigón a partir de imágenes superficiales

Gamze Doğan[1], Ahmet Özkış[2], and Musa Hakan Arslan[3]

ABSTRACT

This study used digital image processing and an artificial neural network (ANN) to determine the compressive strength of concrete in reinforced concrete buildings without coring. First, 32 concrete samples were produced in the laboratory, with different water-to-cement ratios, aggregate types, amounts of binder, compression values applied to fresh concrete, and amounts of additive. Next, the locations of 192 cores were visualized, and the compressive strengths of their corresponding core samples were matched with the surface images of the concrete, which were then digitized by image processing. The digitized images were the input layer, and the training and testing procedures were performed using the ANN as an output layer. After testing, the model was validated in existing reinforced concrete buildings. For the verification process, 20 cores taken from randomly selected concrete buildings were used. Although the results obtained from the samples produced in the laboratory were satisfactory, the success rate of the samples taken from the field was limited. Finally, the findings of this study are compared against the literature on this subject, especially from the last two decades.

Keywords: reinforced concrete, building, digital image processing, intelligent system, compressive strength, experimentation

RESUMEN

En este estudio se utilizó procesamiento de imágenes digitales y una red neuronal artificial (ANN) para determinar la resistencia a la compresión del hormigón en edificios de hormigón armado sin tomar núcleos. Primero, se generaron 32 muestras de concreto en el laboratorio con diferentes proporciones de agua a cemento, tipos de agregado, cantidades de aglutinante, valores de compresión aplicada al concreto fresco y cantidades de aditivo. A continuación, se visualizaron las ubicaciones de 192 núcleos, y las resistencias a la compresión de sus correspondientes muestras se compararon con las imágenes de la superficie del hormigón, que se digitalizaron mediante procesamiento de imágenes. Si las imágenes digitalizadas fueron la capa de entrada, y los procedimientos de entrenamiento y prueba se realizaron utilizando la ANN como capa de salida. Después de las pruebas, el modelo se validó en edificios reales de hormigón armado. Para el proceso de verificación, se utilizaron 20 núcleos tomados de edificios de hormigón seleccionados al azar. Si bien los resultados obtenidos de las muestras producidas en el laboratorio fueron satisfactorios, el porcentaje de éxito de las muestras tomadas en campo fue limitado. Por último, se comparan los hallazgos del estudio con la literatura sobre este tema, especialmente de las últimas dos décadas.

Palabras clave: edificios de hormigón armado, procesamiento de imágenes digitales, sistema inteligente, resistencia a la compresión, experimentación

Received: April 1st, 2022
Accepted: April 10th, 2023

Abbreviation	Meaning
ANN	Artificial neural networks
DIP	Digital Image processing
CS	Compressive strength
RC	Reinforced concrete
f_{cmin}	Minimum compressive strength of concrete
f_{cmean}	Average compressive strength of concrete
s_s	Standard deviation

[1] Faculty of Engineering and Natural Sciences, Department of Civil Engineering, Konya Technical University, Konya 42130, Turkey, gdogan@ktun.edu.tr
[2] Necmettin Erbakan University, Faculty of Engineering, Department of Computer Forensics Engineering, Konya 42090, Turkey, aozkis@erbakan.edu.tr
[3] Faculty of Engineering and Natural Sciences, Department of Civil Engineering, Konya Technical University, Konya 42130, Turkey, mharslan@ktun.edu.tr

Introduction

Determining the compressive strength (CS) of concrete in existing buildings is time-consuming, costly, and complicated. The most precise method for doing so is the destructive method of coring, whose disadvantages include damage to the area from which the core is taken, the loss of section capacity, after-coring repair and modification costs, testing costs, and a delay of at least one day between taking the core and obtaining the CS value.

Building codes – such as ACI-318-19 (2018), TS-500-2000 (2000), and TBEC-2018 (2018) – provide some rules for taking concrete core samples. They must be taken from an existing building if the supervising engineer requires tests to determine the CS of the concrete, and the coring must be done from locations that do not reduce the strength of the structure. Moreover, building codes allow the use of non-destructive testing methods (*e.g.*, surface hardness and sound velocity) for correlation with the concrete coring results, but these alternative methods are less effective than taking core samples. For example, the success rate of the ultrasonic sound velocity method, which is frequently cited in the literature, is known to be only 65-75% (Sbartai *et al*., 2012; Breysse, 2012; Ferreira and Jalali, 2010).

There have been numerous studies involving different methods for determining the CS of concrete, and the success of each method has been assessed in comparison with that reported for the concrete pressure test in the literature (Bogas *et al*., 2013; Sbartai *et al*., 2012; Breysse, 2012; Ferreira and Jalali, 2010; Bingöl and Çavdar, 2018; Thapa *et al*., 2019). It has been established that each method has its own success rate, which is unfortunately inversely related to its ease of application. Therefore, it is highly necessary to devise a method that is both easily applicable and cost-effective while providing results both quickly and as close as possible to those of coring.

In recent years, images of the surfaces of newly produced (Doğan *et al*., 2015, 2017; Al-Kamaki *et al*., 2017; Beskopylny *et al*., 2022; Shiuly *et al*., 2022) or hardened cylinder and cube samples have been taken to calculate the CS of concrete via image processing technology. As an alternative to mechanical methods, image processing technology (Jang *et al*., 2019; Naderpour *et al*., 2018; López *et al*., 2009; Chang *et al*., 2009; Gencturk *et al*., 2014) allows measuring without direct contact with the surface of the material or requiring a complicated and expensive experimental setup.

Unlike previous studies, this study assesses the feasibility of determining the CS of reinforced concrete (RC) in existing buildings not by taking cores but via concrete-surface images analyzed using digital image processing (DIP) and an artificial neural network (ANN). The main objectives of this research are as follows: (i) to develop a new test method that engineers can use with an acceptable accuracy without damaging the structure; (ii) to make it easier to quickly reach results in the most time-consuming part of fieldwork regarding processes such as risk analysis in existing RC buildings and earthquake performance calculations; (iii) to provide significant cost and time savings by ensuring that concrete CS (one of the most critical factors in the behavior of a structure) can be determined both rapidly and economically; (iv) to offer an alternative and innovative method that uses expert systems instead of an uneconomical and time-consuming process that damages the structure (*e.g.*, coring).

Compressive strength (f_c) is one the main parameters of concrete since it directly affects other mechanical parameters. Especially in the last major earthquakes (such as the 2023 Kahramanmaraş-Turkey earthquakes, in which approximately more than 50 000 people died and hundreds of thousands of RC buildings completely collapsed), it has been clearly seen that a low concrete strength may cause structure collapse. The method proposed in this study shows the extent to which concrete strength can be determined in existing RC buildings with an artificial intelligence-based algorithm and without the need for destructive methods. The novelty of this study is the ability to determine the concrete strength detectability ratio from the surface in buildings without taking core samples via a technology used in many engineering problems. This work fills the gap on this subject while showing huge differences between the experimental studies carried out in a laboratory environment and the tests carried out in real buildings.

To this effect, 32 different samples were produced while varying five parameters (water/cement ratio, aggregate type, the amount of binder, the compression to be applied to fresh concrete, and the amount of additive) that affected the CS and surface appearance of the concrete. The locations of 192 cores to be taken from these concrete samples were determined, and these regions were visualized before coring. The CS values of the core samples taken from these regions were matched with the surface images of the concrete, which were digitized via image processing. The DIP images formed the input layer of an ANN, whose output layer was the core CS of the imaged regions. The 192 data were used to train and test the ANN, and the tested model was validated in existing RC buildings. For the verification process, 20 different concrete images taken from randomly selected concrete buildings were used.

A brief literature review

In this section, current studies on concrete CS estimation in the literature are briefly summarized (Table 1). Note that intelligent systems and algorithms have been frequently used in research on concrete samples in recent years.

Digital image processing and artificial neural network

ANNs are a type of machine learning algorithm inspired by the structure and functioning of the human brain. They are designed to recognize patterns and learn from data inputs in

Table 1. Literature survey on the use of intelligent systems in concrete

Researcher / Methods	Brief description	Main findings
Doğan *et al*. (2017) ANN and image processing	A new non-destructive experimental method that uses image processing techniques and ANN	The method showed a very high prediction success (between 97,18 and 99,87%).
Behnood and Golafshani (2018) ANN, MOGWO	A predictive model for the compressive strength of silica fume concrete	A total of 31 non-dominated ANN models on the Pareto front with different architectures and accuracies was achieved. 22 of them had a Pearson correlation coefficient higher than 0,95.
Golafshani *et al*. (2020) ANN, ANFIS, and GWO	A reliable model for the prediction of concrete compressive strength.	Using metaheuristic optimization algorithms in the training phase of ANN and ANFIS can reduce the weakness of classical optimization algorithms and lead to more reliable results.
Kandiri *et al*. (2020) ANN, multi-objective salp swarm algorithm, M5P model tree	A database for the compressive strength of concrete was elaborated via GGBFS, modeling the compressive strength of concrete with ground granulated blast furnace slag (GGBFS) using machine learning.	19 ANN models with various structures and precisions were obtained, which provides alternatives according to the required simplicity and complexity.
Feng *et al*. (2020) Adaptive boosting approach	The AdaBoost algorithm was adopted to predict the compressive strength of concrete.	The AdaBoost model can accurately and efficiently predict the compressive strength of concrete with given input variables.
Omran *et al*. (2016) Multilayer perceptron, support vector machines, Gaussian processes regression, M5P, REPTree, M5-Rules, and decision stump, additive regression, and bagging	A comparison of the performance of nine data mining models in predicting the compressive strength of a new type of concrete containing three alternative materials (fly ash, haydite lightweight aggregate, and Portland limestone cement).	The analytical results show that, with appropriate parameter settings, all of these models except decision stump can achieve an acceptable prediction performance.
Yaseen *et al*. (2018) Extreme Learning Machine (ELM)	The regression-based soft computing model called *Extreme Learning Machine* was used for predicting the compressive strength of lightweight foamed concrete.	Four models achieved superior predictive capability for the effects of various influential input variables on the compressive strength of concrete.
Dao *et al*. (2019) ANFIS, ANN	Two artificial intelligence approaches, ANFIS and ANN, were used to predict the compressive strength of GPC aggregates.	Both ANN and ANFIS models have strong potential for predicting the compressive strength of GPC.
Bui *et al*. (2018) modified firefly algorithm (MFA), ANN	An expert system to predict the compressive and tensile strength of HPC.	Rapid convergence to an optimal value is a key advantage of the MFA-ANN hybrid expert system, facilitated by the systematic updating, memorization, and optimization of firefly details along with weight and bias parameters.
Başyiğit *et al*. (2012)	IP methods.	The compressive strength of concrete was successfully estimated through the use of IP, demonstrating an impressive accuracy rate of 94,8%.
Waris *et al*. (2022)	Combined use of image pro-cess-ing, ANN and ANFIS computational tech-niques.	The accuracy achieved through the combination of IP and ANN stands at an impressive 99,7%, an accuracy of 97,8% was obtained with IP and ANFIS.

Source: Authors

a way that is similar to how the humans process information. An ANN consists of a large number of interconnected processing nodes, which are organized in layers. Each node receives an input from other nodes or from external data, processes it via a mathematical function, and then passes the output to other nodes in the network. The connections between the nodes are weighted, which means that some inputs are more important than others. During the training process, the network is presented with a large number of input-output pairs, and the weights of the connections between the nodes are adjusted in order to minimize the difference between the actual output and the desired output. This is typically done using an optimization algorithm such as a gradient descent.

ANNs are used in a wide variety of applications, including image and speech recognition, natural language processing, and predictive modeling. They have proven to be particularly effective in applications where the input data is high-dimensional and complex, and where traditional rule-based approaches are difficult to apply.

Digital image processing means processing images via computers or other digital devices. This process uses a range of mathematical, algorithmic, and hardware techniques to capture, process, analyze, refine, and ultimately make images more useful. Digital image processing is used in a variety of industries, such as medicine, security, computer vision, robotics, manufacturing, remote sensing, and entertainment. This technology is used to take image data, make them more meaningful, and facilitate analysis. Examples of this include X-ray images, air traffic control systems, image-based sensors in automated vehicles, *etc*.

Image processing involves emulating, in a computer environment, the visual mechanism of the human eye and the image-interpretation mechanism of the brain. With this technique, certain information that cannot be accessed directly from an image of either an entire object or a region of it can be accessed indirectly. An image can be defined by the function f (x, y) with values in the xy coordinate plane, each of which represents the color value of the image at those coordinates. The color values of monochrome images are defined either as black and white (0 and 1, respectively) or as grey levels (0-255) (González *et al*., 2004). Continuous density values in continuous space are expressed as discrete values using a digitization method, thereby allowing images to be displayed, improved, segmented, and transformed by computers (Easton Jr., 2010). This process is known as DIP, which, in this study was performed using the MATLAB software (MATrix LABoratory).

Materials and methods

This section explains the production and acquisition stages of the core sample data and the application of DIP and the ANN, which constitutes the analytical part of this study.

Training and production of the test set

First, a dataset was created for the training and testing procedures. Therefore, different concrete samples were produced with binary changes in five different parameters in a laboratory setting. The parameters and their ranges are presented in Table 2. Each parameter affected both the surface appearance and the mechanical properties of the concrete.

Table 2. Brief description of the parameters

Parameter Number	Parameter	Parameter properties
1	Water/ cement ratio	0.93-0.60
2	Aggregate	Normal aggregate – fine sand additive aggregate
3	Compaction	Yes/No
4	Standard curing	Applied – implemented
5	Admixture materials (plasticizer)	Yes/No

The 32 concrete samples were produced with the aim of taking a total of 192 core samples (six from each concrete sample). Figure 1 shows a schematic of the dimensions of the concrete samples, which were prepared according to the calculated mixture ratios, poured into rectangular molds and then grouped in sets (Figure 2). Table 3 shows the mixing ratio for each concrete sample. The cement used was selected according to TS-EN-197-1 (2012). Because the desired target concrete strengths were in the range of 15-35 MPa, the cement dosage used in the study varied. Inel *et al*. (2008) showed that the CS of the concrete in the RC buildings that account for a significant portion of the existing building stock in Turkey is quite variable. Therefore, half of the concrete samples prepared in the present study were subjected to TS EN 206 (2014), while the other half were not subjected to compression. Similarly, half of the samples were subjected to standard curing conditions according to TS EN 206 (2014), while the other half were not. The additive Sikament-MR 50SR was used in proportions of up to 1,0% by weight of cement

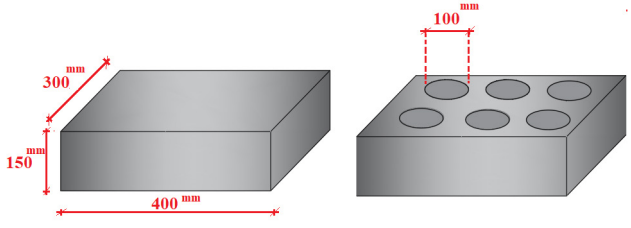

Figure 1. Schematic of the produced concrete masses
Source: Authors

Table 3. General properties of parameters.

Parameter Number	Parameters		Variation range	
			Code:1	Code:0
1	Cement (CEM I 42.5)		220 kg/m³	360 kg/m³
	Water		205 kg/m³	209 kg/m³
	Water/cement ratio		0.60	0,93
2	Aggregate granulite (Dmax=22,4 mm)	15-22,5	230	200
		0-5 Sand	510	675
		8-16	600	600
		0-5 Sand	510	500
3	Compaction		Complying with TS-EN 206	Non-complying TS-EN 206
4	Standard curing		Complying with TS-EN 206	Non-complying TS-EN 206
5	Admixture materials (plasticizer)		Sikament-MR 50SR (Complying with TS-EN 934-2)	No

Figure 2. Produced concrete masses
Source: Authors

28 days after the concrete samples were made, concrete faces were taken so that the cores could be taken. Having cleaned the surfaces of the concrete samples, the regions from which the cores were to be taken were marked and visualized under the same conditions. The surface images were taken at a constant distance under the same light intensity and with a fixed angle and resolution ratio. After imaging the locations of the cores, the latter were taken from the concrete samples. The imaging and coring process is shown schematically in Figure 3, and the coring process and core samples in the laboratory are shown in Figure 4. The core length-to-diameter ratio was set at 1,5. The process of making and breaking the cores was compliant with ASTM C42 (2016), TS EN 13791 (2010), and TS EN 12504-1 (2010). In the experiments on the core samples, a uniaxial vertical loading test was carried out by means of an automatic controlled hydraulic press with a vertical loading capacity of 3 000 kN. Table 4 presents the properties of the samples and their minimum and maximum strengths. The test results show that the core CS values were in the range of 15,51-41,84 MPa (fc).

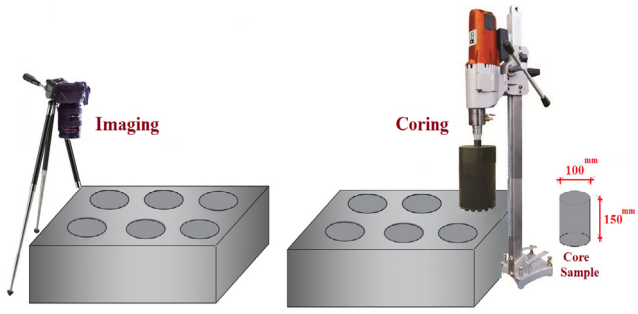

Figure 3. Imaging and coring of a concrete mass
Source: Authors

Figure 4. Data preparation: a) coring process; b) core samples whose surface images were taken
Source: Authors

Obtaining a validation set

To verify the results from the concrete samples to be used in the intelligent system for training and testing purposes, a validation dataset was created independently from the dataset. To create the validation set, six different existing RC buildings from different years in Turkey were randomly selected, and core sampling was carried out on them. The fact that they were all low-rise buildings is related to the distribution of the building stock in the selected region. Figure 5 shows the buildings from which the cores were taken, the year in which each building was constructed, and the number of cores taken from each building.

(a) (b)

(c) (d) (e) (f)

Figure 5. Construction years of the buildings and the number of core samples taken from each one: a) building-1 (2001, three concrete cores); b) building-2 (2009, five concrete cores); c) building-3 (2011, three concrete cores); d) building-4 (2017, three concrete cores); e) building-5 (1989, three concrete cores); f) building-6, industrial structure (2015, three concrete cores)
Source: Authors

Table 4. Sample types, parameter codes, and strength ranges

Sample name*	Sample number*	W/C	Aggregate	Compaction	Standard curing	Admixture materials	fc (MPa)	
		Codes					min	max
A1	6	1	1	1	1	1	26.17	34.33
A2	6	0	1	1	1	1	23.56	33.99
A3	6	0	0	1	1	1	15.51	33.80
A4	6	0	0	0	1	1	20.85	29.48
B1	6	0	0	0	0	1	17.64	29.75
B2	6	0	0	0	0	0	21.65	32.00
B3	6	1	0	1	1	1	18.45	29.03
B4	6	1	1	0	1	1	23.56	30.21
C1	6	1	1	1	0	1	20.70	27.04
C2	6	1	1	1	1	0	17.19	21.25
C3	6	0	0	1	0	1	18.16	27.10
C4	6	0	1	0	1	0	18.26	23.67
D1	6	1	0	0	1	1	33.59	36.82
D2	6	1	0	0	0	1	31.41	41.84
D3	6	1	0	0	0	0	25.08	36.20
D4	6	1	1	0	0	1	26.20	33.95
E1	6	1	1	0	0	0	30.01	36.23
E2	6	1	1	1	0	0	25.14	36.17
E3	6	0	1	0	0	0	25.15	35.39
E4	6	0	1	1	0	0	28.88	32.93
G1	6	0	1	1	1	0	32.77	35.29
G2	6	0	0	1	0	0	27.89	35.46
G3	6	0	0	1	1	0	18.31	32.31
G4	6	0	1	1	0	1	26.80	36.86
H1	6	0	0	0	1	0	29.78	36.20
H2	6	1	1	0	1	0	28.39	34.82
H3	6	0	1	0	0	1	20.60	38.95
H4	6	0	1	0	1	1	27.25	35.88
K1	6	1	0	1	0	0	22.42	37.32
K2	6	1	0	1	0	1	34.11	41.84
K3	6	1	0	1	1	0	27.33	36.26
K4	6	1	0	0	1	0	30.57	37.44

*: A total of 8 different groups (A-K), 4 different types (1-2-3 and 4) and 192 different samples in each group

Figure 6. Coring from buildings and imaging of cores
Source: Authors

The photographs of the core surfaces were taken at a fixed distance, and the CS values of the cores was then determined by subjecting them to a uniaxial vertical loading test. Because the buildings that were used were constructed in different years and with different classes of concrete, the strengths of the concrete samples were in the range of 13,41-35,63 MPa.

The process of obtaining the cores from the RC structures and the images of the cored samples is shown step by step in Figure 5. First, the areas in the RC elements from which the cores were to be taken were determined, for which an X-ray device was used, in order to identify any reinforcements inside the elements (Figure 6a). Having determined a non-reinforced area in an RC element, the area to be cored was prepared for imaging (Figure 6b). To obtain an image of the concrete surface in the coring area, the layers of paint and plaster on the column were dug through to reach the plain concrete surface (Figure 6c). The camera was secured on a tripod to obtain an image from a fixed distance (40 cm away) (Figure 6d). A coring device was used to cut a core sample from the RC column (Figure 6d and 6f), and the core sample was also photographed. Here, the aim was to determine whether the photographs of the core samples before cutting yield different results from those after cutting (Figure 6g). The core samples were then brought to the laboratory, and their CS values were measured in a uniaxial pressure test using a hydraulic press (Figure 6h).

Analytical work for the core samples

In this study, the concrete dataset used for training and the test data of the algorithm comprised the 192 concrete samples obtained by taking six cores from 32 different concrete types. Because the CS of the concrete was a random variable, the frequency factor was taken to be 1,28 according to the probability distribution of the concrete CS (assuming an exceedance probability of 10%). The standard deviation of the distribution was calculated, and elements with either very low or very high strength were removed from the 192 concrete data (Figure 7). This process left 160 concrete samples in the data set.

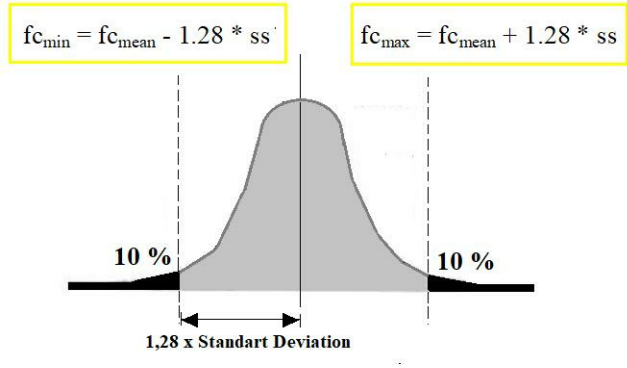

Figure 7. Elimination of the data set
Source: Authors

A 779 × 1 069 pixel image was taken from each of the 160 concrete samples and then converted to grey scale. Then, the average, standard deviation and median values of all the columns in each of the concrete images were calculated, thus yielding data comprising 3 × 1 069 = 3 207 pixels for each concrete image. Thus, a 160 × 3 207 pixel dataset was created for the 160 concrete samples.

The fact that the number of inputs for the ANN was as large as 3 207 had a negative effect on the training process in terms of time and calculation. To counter that problem, a feature-extraction algorithm based on principal components analysis (PCA) was used to reduce the number of properties

for each concrete sample to 50, resulting in a data set in the form of a 160 × 50 matrix. The 160 data were divided into 128 training and 32 testing data to perform five-fold cross-validation (a separate 32-group for each cross-validation process was divided as testing data).

In this study, the Levenberg-Marquardt ANN model was used, with 50 neurons in the input layer, 52 in the interlayer, and one in the output layer (Figure 8). Table 5 presents the values of the other network parameters. In the literature, commonly used activation functions are the linear, step, sigmoid, Gaussian, and hyperbolic tangent. In this study, the selected activation function was the (logarithmic) sigmoid one. The ANN training process was terminated either after 50 iterations or if the training error became less than 10-6. The latter tended to happen after 10 to 12 epochs (Figure 9).

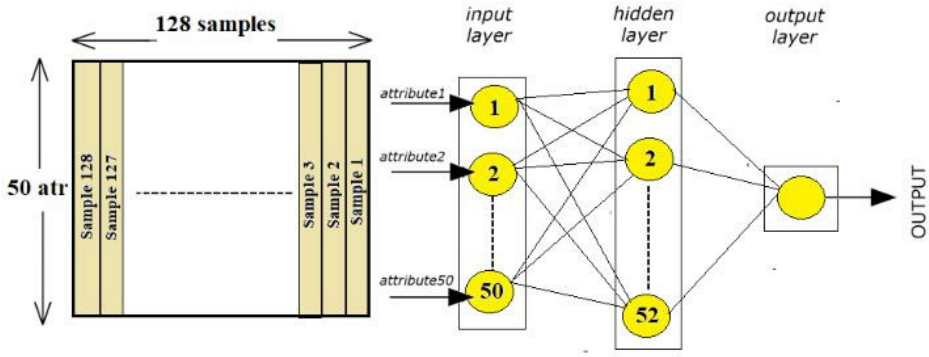

Figure 8. ANN structure used for training
Source: Authors

Table 5. ANN model and used parameters

Properties	Variation range
Activation function	Logarithmic sigmoid
Epoch number	50
Stopping criterion	1e-6
Maximum validation error	6
Minimum error tolerance	1e-10
Marquardt setting parameter	0,005
Marquardt setting parameters reduction factor	0,1
Marquardt setting parameters growth factor	10
Marquardt setting parameters max value	1e10
How many epochs will be updated in the image	50

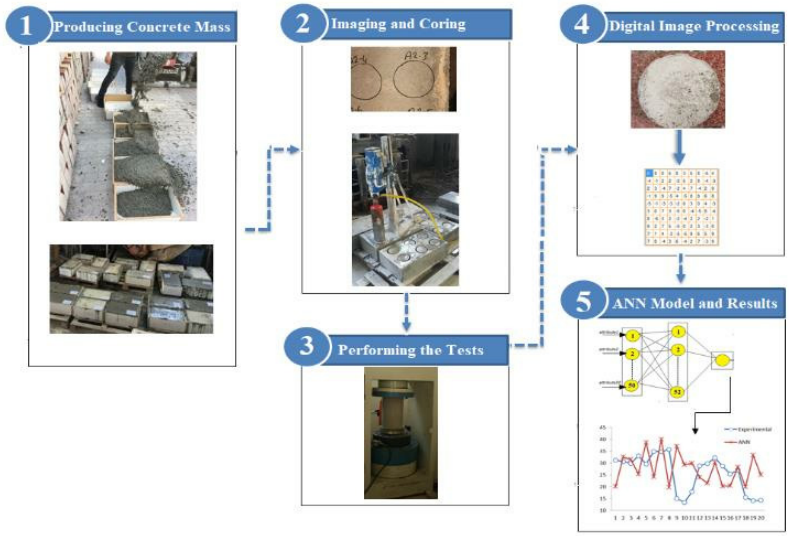

Figure 9. Process steps
Source: Authors

Results

The 160 data were divided into 128 training and 32 testing data to perform different five-fold cross-validations. For each cross-validation process, a separate group of 32 was determined as the testing data. After completing the training, the estimated values produced by the network for the 32 testing data were compared against the expected values. If the margin of error was less than 5% (between the estimate and the expected value), then the value was considered to be correct. The margin of error was then increased by 5%, and the correct predicted value ratio was determined. In light of the fact that destructive test methods include error levels of 30-40%, Table 6 shows (i) an accuracy of 73,6% with a 30% margin of error and (ii) an accuracy of 86,4% with a 40% margin of error. Table 6 shows the accuracy and error ratios, and Figure 10 shows a graph of the mean accuracy of the five-fold cross-validation results.

After training and testing the ANN model, it was applied to the validation set. The laboratory results for the cores obtained from the buildings were compared to those obtained from the ANN. Table 7 lists the experimental CS values obtained from the core samples and the estimated CS values obtained via DIP and the ANN. Figure 11 compares the results graphically.

Table 6. Error ratio (%) – Accuracy rate (%)

Error ratio (%)	Accuracy Rate (%)					Average accuracy rate (%)
	Cross fold 1	Cross fold 2	Cross fold 3	Cross fold 4	Cross fold 5	
30%	81	53	**84**	72	78	73.6
35%	84	69	**88**	84	78	80.6
40%	**94**	72	**94**	84	88	86.4

Source: Authors

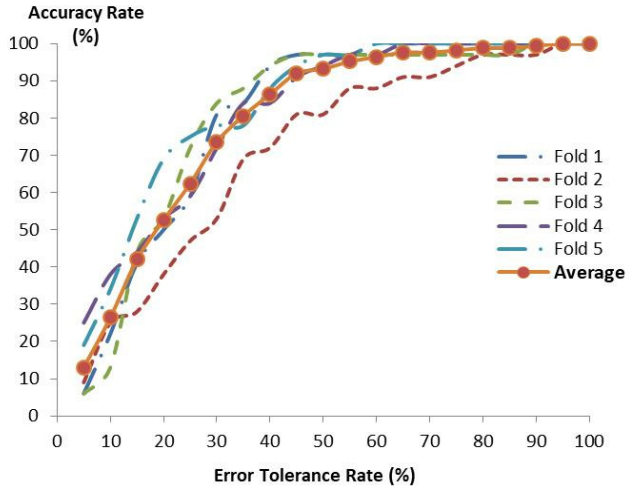

Figure 10. Accuracy of 5-fold cross validation results for the test set
Source: Authors

Table 7. Compressive strength values (MPa) of the core samples (experimental, EXP – analytical, ANN)

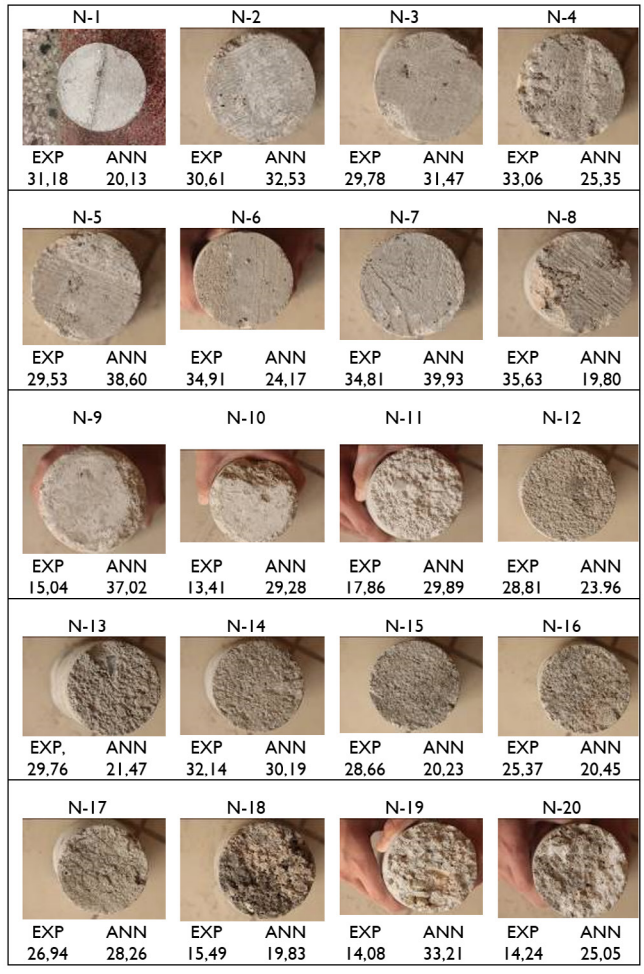

Source: Authors

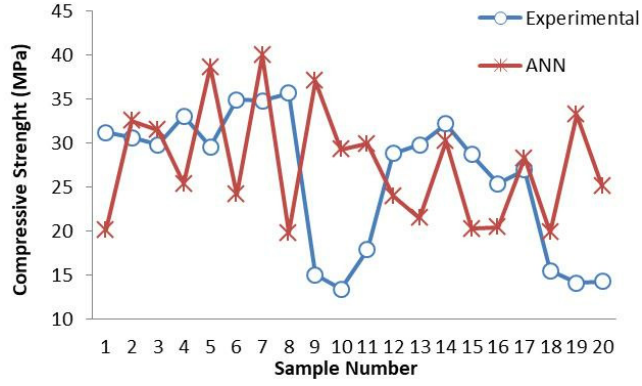

Figure 11. Compressive strength comparison chart for real buildings (experimental-ANN)
Source: Authors

Table 7 shows that, when the estimated and measured CS values (MPa) of the core samples are compared, some are close, and the results of different experiments were reached in most samples.

Discussion

The results obtained in this study are somewhat poor when compared to similar studies in the literature (such as Başyiğit *et al*., 2012, and Waris *et al*., 2022, who found success rates close to 95% in their studies). However, the main reason for this is that the images were not taken from the surfaces of the concrete samples, which were tested by cutting (slicing) in a laboratory environment. However, there is not much chance of such a production being practically carried out in field studies. Although the results obtained for the laboratory-produced concrete samples are quite satisfactory, the success for the fieldwork samples in the validation set was limited. The proposed method had a success percentage of less than 50% for these samples. In this case, the training, testing, and validation set yield quite different results. The fact is that the laboratory-produced samples do not fully reflect the concrete in the real RC buildings; the images of the cores taken from the existing buildings are different from those of the concrete samples obtained in the laboratory. The results were affected by changes in the image quality of the samples and the difference in the amount of light. The reason for this was fluctuations in the images due to the roughness of the core samples. In this study, because the prediction success for the existing buildings was low, the authors conclude that using only surface images is insufficient for estimating the CS of concrete. It is thought that using images of internal concrete surfaces revealed by cutting the core samples will increase the success of predicting the CS. Similarly, high success was achieved from new concrete cylinder and cube samples (Jang *et al*., 2019) taken using the appropriate method, while the success in core samples was not satisfactory.

According to the results obtained in previous studies involving artificial intelligence and examples of various engineering problems, this study's results are poor. The main reasons for this are given below.

1. Although a comprehensive dataset was prepared for the laboratory test and a wide parameter group was used, the surface images obtained in the laboratory did not represent the results obtained from a real structure.

2. In the literature, the training and testing datasets are similar in many engineering problems to which artificial intelligence is applied. Moreover, in many applications, the testing and training data are produced in a laboratory environment, in which case the results tend to be more accurate. However, in a branch of science such as civil engineering, where laboratory and field conditions vary greatly, it would not be right to perform evaluations only from laboratory results. The results show how field and laboratory studies differ in structural engineering. Sufficient engineering service (proper supervision to reduce human error) is also vital, especially during concrete production.

3. There are many parameters affecting concrete CS. In this study, parameters such as the water/cement ratio, aggregate type, compaction, curing, and admixture materials (plasticizer) were used to create the dataset. 28 days after the production of concrete in the laboratory, the surface images were taken, and compression tests were conducted. On the other hand, the construction years of the randomly selected buildings in the field study vary between 1989 and 2017. Here, it can be said that the image data changed a lot, as the carbonation formed on the concrete surface changes depending on the time. This is thought to be the most crucial reason that affects the results.

4. Another cause is surface defects due to the type of RC formwork, design errors, and the improper use of formwork oils. In practice, mold surfaces tend to be made of wood, plywood, metal, or plastic, and impermeable mold surfaces that do not absorb water cause gaps and possibly surface roughness on the concrete.

5. In the core application of this study, the plaster was scraped before the concrete surface was photographed. To remove dust, it would be useful to clean the photographed area using either compressed air or pressurized water.

6. The direction in which concrete is cast also affects its placement and therefore its CS. The samples produced in the laboratory were cast horizontally, whereas the real building samples that were tested were taken from columns that had been cast vertically.

7. While extracting the concrete core samples, the possible reinforcement bar parts in the core samples can significantly change the compression test results.

8. Increasing the dataset used in the study will positively affect the results. However, the fact that the surface image quality is standard (i.e., photographed distance, light level, resolution, shading) is fundamental. These parameters affect the result.

9. In the study, in the image analysis step, a region of 779 x 1 069 pixels was taken from the concrete core image. The whole area of the core affecting compressive strength was not used.

10. Regarding the core samples taken from the RC in the buildings, parts of the reinforcement bars that could have been in the core samples would have significantly changed the results of the compression test.

In the literature, for the determination of concrete CS, the success rates of the methods proposed in comparison with the core test results do not exceed this level. When evaluated from this point of view, it can be said that only the analyses made on laboratory samples are satisfactory. The authors

think that a combined non-destructive testing method will be an important tool for determining CS in the future, not only with images, but also with other parameters such as sound permeability and surface hardness.

Conclusions

In this study, an experimental and analytical study was conducted using DIP and ANN together to determine the compressive strength of concrete in existing reinforced concrete buildings without cores. According to the study, the findings presented in the following items were reached.

1. The laboratory samples obtained an accuracy of 73,6% with a 30% margin of error and an accuracy of 86,4% with a 40% margin.

2. In this study, the test procedures had a high success rate, which was lower for random samples collected from real buildings.

3. The success rate of other non-destructive testing methods such as surface hardness and sound absorption is known to be only 65-75% The prediction success of the proposed method in this study is slightly better than that of traditional methods.

Acknowledgements

This study was carried out within the framework of research project no. 16401038, supported by the Selcuk University, Scientific Research Projects Coordination.

Conflicts of interest

The authors declare that they have no known competing financial interests or personal relationships that could have appeared to influence the work reported in this paper.

CRediT author statement

All authors: conceptualization, methodology, software, validation, formal analysis, investigation, writing (original draft, writing, review, and editing), data curation.

References

ACI 318-19 (2018). *Building code requirements for structural concrete and commentary*. American Concrete Institute. https://www.usb.ac.ir/FileStaff/5526_2020-1-25-11-12-7.pdf

Al-Kamaki, Y. S. S., Al-Mahaidi, R., and Bennetts, I. (2017). Strain efficiency of carbon fibre reinforced polymer-confined RC columns. *Journal Of Duhok University*, *20*(1), 484-497. https://Doi.Org/10.26682/Sjuod.2017.20.1.43

ASTM C42/C42M (2016). *Standard test method for obtaining and testing drilled cores and sawed beams of concrete*. ASTM. https://www.astm.org/c0042_c0042m-13.html

Başyiğit C., Çomak B., Kiliçarslan S., and Üncü I. S. (2012). Assessment of concrete compressive strength by image processing technique. *Construction and Building Materials, 37*, 526-532. https://doi.org/10.1016/j.conbuildmat.2012.07.055

Behnood, A., and Golafshani E. M., 2018, Predicting the compressive strength of silica fume concrete using hybrid artificial neural network with multi-objective grey wolves, *Journal of Cleaner Production*, *202*, 54-64. https://doi.org/10.1016/j.jclepro.2018.08.065

Beskopylny, A. N., Stel'makh, S. A., Shcherban', E. M., Mailyan, L. R., Meskhi, B., Razveeva, I., Chernil'nik, A., and Beskopylny, N. (2022). Concrete strength prediction using machine learning methods CatBoost, k-Nearest Neighbors, Support Vector Regression. *Applied Science, 12*, 10864. https://doi.org/10.3390/app122110864

Bingöl, S., and Çavdar, A. (2016). *A new nomogram proposal to determine concrete compressive strength by combined nondestructive testing methods. Research in Nondestructive Evaluation, 29*(1), 1-17. https://www.tandfonline.com/doi/abs/10.1080/09349847.2016.1195466

Bogas J. A., Gomes, M. G., and Gomes, A. (2013). *Compressive strength evaluation of structural lightweight concrete by non-destructive ultrasonic pulse velocity method*. *Ultrasonics, 53*, 962-97. https://pubmed.ncbi.nlm.nih.gov/23351273/

Breysse, D. (2012). Nondestructive evaluation of concrete strength: An historical review and a new perspective by combining NDT methods. *Construction and Building Materials, 33*, 139-163, https://doi.org/10.1016/j.conbuildmat.2011.12.103

Bui, D. K., Nguyen, T., Chou, J. S., Xuan, H. N., and Ngo T. C. (2018). A modified firefly algorithm-artificial neural network expert system for predicting compressive and tensile strength of high-performance concrete. *Construction and Building Materials*, *180*, 320-333. https://doi.org/10.1016/j.conbuildmat.2018.05.201

Chang, C. W., Chen, P. H., and Lien, H. S. (2009). Evaluation of residual stress in pre-stressed concrete material by digital image processing photoelastic coating and hole drilling method. *Measurement, 42*(4), 552-558. https://doi.org/10.1016/j.measurement.2008.10.004

Dao, D. V., Ly, H. B., Trinh, S. H., Le, T. T., and Pham, B. T. (2019). Artificial intelligence approaches for prediction of compressive strength of geopolymer concrete. *Materials*, *12*(6), 983. https://doi.org/10.3390/ma12060983

Doğan, G., Arslan, M. H., and Ceylan, M. (2015). Statistical feature extraction based on an ANN approach for estimating the compressive strength of concrete. *Neural Network World*, *25*(3), 301-318. http://www.nnw.cz/doi/2015/NNW.2015.25.016.pdf

Doğan, G., Arslan, M. H., and Ceylan, M. (2017).Concrete compressive strength detection using image processing based new test method. *Measurement, 109*, 137-148. https://doi.org/10.1016/j.measurement.2017.05.051

Easton Jr., R. L. (2010). *Fundamentals of digital image processing*. https://www.cis.rit.edu/class/simg361/Notes_11222010.pdf

Feng, D. C., Liu, Z. T., Wang, X. D., Chen, Y., Chang, J. Q., Wei D. F., and Jiang, Z. M. (2020). Machine learning-based compressive strength prediction for concrete: An adaptive boosting approach, *Construction and Building Materials*, *230*, 117000. https://doi.org/10.1016/j.conbuildmat.2019.117000

Ferreira, R. M., and Jalali, S. (2010). NDT measurements for the prediction of 28-day compressive strength. *NDT&E International, 43*, 55-61. https://doi.org/10.1016/j.ndteint.2009.09.003

Gencturk, B., Hossain, K., Kapadia, A., Labib, E., and Mo, Y. L. (2014). Use of digital image correlation technique in full-scale testing of prestressed concrete structures. *Measurement, 47*, 505-515. http://dx.doi.org/10.1016/j.measurement.2013.09.018.

González, R. C., Eddins, S. L., and Woods, R. E. (2004). *Digital image processing using MATLAB* (vol. 624). Pearson-Prentice-Hall.

Golafshani, E. M, Behnood, A., and Arashpour, M. (2020). Predicting the compressive strength of normal and high-performance concretes using ANN and ANFIS hybridized with grey wolf optimizer. *Construction and Building Materials*, *232*, 117266. https://doi.org/10.1016/j.conbuildmat.2019.117266

Inel, M., Bilgin, H., and Ozmen, H. B. (2008). Seismic capacity evaluation of school buildings in Turkey. *Structures & Buildings, 161*(3),147-159. https://doi.org/10.12989/sem.2008.30.5.535.

Jang, Y., Ahn, Y., and Kim, H. Y. (2019). Estimating compressive strength of concrete using deep convolutional neural networks with digital microscope images. *Journal of Computing in Civil Engineering, 33*(3), 0000837. https://ascelibrary.org/doi/10.1061/%28ASCE%29CP.1943-5487.0000837

Kandiri, A., Golafshani, E. M., and Behnood, A. (2020). Estimation of the compressive strength of concretes containing ground granulated blast furnace slag using hybridized multi-objective ANN and salp swarm algorithm. *Construction and Building Materials*, *248*, 118676. https://doi.org/10.1016/j.conbuildmat.2020.118676

López, M., Kahn, L. F., and Kurtis, K. E. (2009). Characterization of elastic and time-dependent deformations in high performance light weight concrete by image analysis. *Cement and Concrete Research, 39*, 610-619. http://dx.doi.org/10.1016/j.cemconres.2009.03.015

Naderpour, H., Rafiean, A. H., and Fakharian, P. (2018). Compressive strength prediction of environmentally friendly concrete using artificial neural networks. *Journal of Building Engineering, 16*, 213-219. https://doi.org/10.1016/j.jobe.2018.01.007

Omran, B. O., Chen, Q., and Jin, R. (2016). Comparison of data mining techniques for predicting compressive strength of environmentally friendly concrete. *Journal of Computing in Civil Engineering*, *30*(6), 0000596. https://doi.org/10.1061/(ASCE)CP.1943-5487.0000596

Sbartai, A. M., Breysse, D., Larget, M., and Balayssac, J. P. (2012). Combining NDT techniques for improved evaluation of concrete properties. *Cement and Concrete Composites, 34*, 725-733. https://doi.org/10.1016/j.cemconcomp.2012.03.005

Shiuly, A., Dutta, D., and Mondal, A. (2022). Assessing compressive strengths of mortar and concrete from digital images by machine learning techniques. *Frontiers of Structural and Civil Engineering, 16*, 347-358. https://doi.org/10.1007/s11709-022-0819-z

Thapa, S., Halder, L., and Dutta, S. C. (2019). *Evaluation of concrete made with stone and brick aggregate using non-destructive testing. Munucipal Engineer*, *174*(1), 43-50. https://doi.org/10.1680/jmuen.18.00030

TBEC-2018 (2018). *Turkey building earthquake code*. Ministry of the Interior, Disaster and Emergency Management Authority.

TS EN 197-1 (2012). Cement- Part 1: *Compositions and conformity criteria for common cements*. TSE.

TS EN 206- (2002). Concrete – Part 1: *Specification, performance, production and conformity*. TSE.

TS EN 12504-1 (2010). *Testing concrete in structures – Part 1: Cored specimens – taking, examining and testing in compression*. TSE.

TS EN 13791 (2010). *Assessment of in-situ compressive strength in structures and precast concrete components*. TSE.

TS-500 (2000). *Turkish standards, design and construction rules of concrete*. TSE.

Waris, M. I., Plevris, V., Mir, J., Chairman, N., and Ahmad, A. (2022). An alternative approach for measuring the mechanical properties of hybrid concrete through image processing and machine learning. *Construction and Building Materials*, *328*, 12689. https://doi.org/10.1016/j.conbuildmat.2022.126899

Yaseen, Z. M., Deo, R. C., Hilal, A., Abd, A. M., Cornejo Bueno, L., Salcedo-Sanz, S., and Nehdi, M. L. (2018) Predicting Compressive Strength of Lightweight Foamed Concrete Using Extreme Learning Machine Model. *Advances in Engineering Software*, *115*, 112-125. https://doi.org/10.1016/j.advengsoft.2017.09.004